Food Research International 105 (2018) 548–555

Contents lists available at ScienceDirect

Food Research International

journal homepage: www.elsevier.com/locate/foodres

Bubbles in noodle dough: Characterization by X-ray microtomography

R.-M. Guillermic[a], F. Koksel[b], X. Sun[b], D.W. Hatcher[b,c], M.T. Nickerson[d], G.S. Belev[e,1], M.A. Webb[e], J.H. Page[a], M.G. Scanlon[b,*]

[a] Department of Physics & Astronomy, University of Manitoba, Winnipeg, Manitoba R3T 2N2, Canada
[b] Department of Food & Human Nutritional Sciences, University of Manitoba, Winnipeg, Manitoba R3T 2N2, Canada
[c] Canadian Grain Commission, Grain Research Laboratory, 1404-303 Main St., Winnipeg, Manitoba R3C 3G8, Canada
[d] Department of Food and Bioproduct Sciences, University of Saskatchewan, 51 Campus Drive, Saskatoon, SK, Canada
[e] Canadian Light Source Inc., 44 Innovation Boulevard, Saskatoon, SK, Canada

ARTICLE INFO

Keywords:
X-ray microtomography
Synchrotron source
Noodle dough
Bubble size distribution
Bubble orientation
Work input

ABSTRACT

Bubbles, found in a huge variety of food products, are known to afford desirable quality attributes, especially those related to texture, mouthfeel and taste. However, the presence of bubbles and their effects on wheat flour noodles is an aspect that has been, until now, largely overlooked, despite the positive and negative connotations of bubbly inclusions on Asian noodle quality. X-rays from a synchrotron source (Biomedical Imaging and Therapy facility at the Canadian Light Source) were used to rapidly and non-destructively acquire tomographic images of noodle dough. Appropriate image analysis protocols were used to determine the bubble size distribution, the orientation of bubbles, and their position within the dough sheet. The effect of processing (one or multiple lamination steps) on bubble properties in the dough that was subsequently sheeted (gradual elongation and reduction in thickness) was investigated. Bubble size distributions, well captured by lognormal distribution function, showed that the lamination process induced bubble entrapment and reduction in bubble size. Bubbles were found to be flat, elongated and oriented in the sheeting direction, this effect being less for doughs laminated ten times (90° rotations between lamination steps). Interestingly, a gradient in concentration of bubbles within the dough sheet was found from the noodle core to the sheet edges. Aging effects were also apparent. This first non-destructive study of bubbles in wheat-flour noodle dough provides a more complete knowledge of the dough sheet's internal structure, and how it originates via processing, and this has repercussions on the overall quality of Asian noodles.

1. Introduction

Asian noodle quality for the consumer is largely determined by the texture and mouth feel of the product (Hou, Otsubo, Okuso, & Shen, 2010; Ross, 2006; Smewing, 2016). In optimizing noodle texture, a good number of studies have focused on the influence of the composition of the noodle dough (Diep et al., 2014; Fu, 2008; Hatcher et al., 2014; Miskelly & Moss, 1985; Ross & Crosbie, 2010) or the work input during noodle making (Edwards, Scanlon, Kruger, & Dexter, 1996; Hatcher & Anderson, 2007). However, the influence of bubbles on noodle properties has not been investigated, despite some researchers mentioning the possibility of the presence of bubbles (Bellido & Hatcher, 2010; Hatcher, Bellido, & Anderson, 2009; Salimi-Khorshidi, 2016), and substantial industrial interest in how vacuum mixing affects noodle rheology and texture (Li et al., 2014; Li et al., 2016; Liu et al., 2015).

Bubbles in food are important for two reasons. Firstly, they are known to contribute to good mouthfeel and texture in many foods (Campbell, Scanlon, & Pyle, 2008; Campbell, Webb, Pandiella, & Niranjan, 1999). In bread making for example, the bubble distribution is strongly affected by the rheological properties of the dough (Bellido, Scanlon, Page, & Hallgrimsson, 2006) and the bubbles in turn affect dough rheology (Chin, Martin, & Campbell, 2005); bubbles also govern the quality of the resulting product (Baker & Mize, 1941; Campbell, Rielly, Fryer, & Sadd, 1998; Scanlon & Zghal, 2001). Secondly, bubbles represent a separate phase within the food material, which can negatively influence the quality of the food product. For example, vacuum mixing of pasta dough is important for product appearance because of the reduction in bubble numbers that occurs (Dawe, Johnston, & Dintheer, 2001). In addition, since the majority of both pasta (Johnston & Dintheer, 2001) and noodle (Hou et al., 2010) products are dried to attain shelf-stability, bubbles can be problematic since they represent

* Corresponding author.
E-mail address: scanlon@cc.umanitoba.ca (M.G. Scanlon).
[1] Current address: Department of Electrical and Computer Engineering, University of Saskatchewan, 57 Campus Drive, Saskatoon, SK, Canada.

https://doi.org/10.1016/j.foodres.2017.11.050
Received 31 August 2017; Received in revised form 9 November 2017; Accepted 19 November 2017
Available online 22 November 2017

discontinuities in the noodle dough matrix from which uneven thermohygroscopic stresses can emanate during drying (Inazu, Iwasaki, & Furuta, 2005; Mercier, Mondor, Moresoli, Villeneuve, & Marcos, 2016); the resulting checking that develops during distribution and retailing is perceived negatively by consumers (Inazu et al., 2005; Smewing, 2016).

Because dough products are not transparent, bubbles cannot be observed by direct visual observation techniques, and preparative techniques for electron microscopy thwart accurate determinations of bubble distributions. X-Ray microtomography is a method that has been successfully used for bread dough products to non-invasively measure bubble size distributions and their evolution over time (Babin, Della Valle, Dendievel, Lourdin, & Salvo, 2007; Falcone et al., 2006; Koksel, Aritan, Strybulevych, Page, & Scanlon, 2016; Turbin-Orger et al., 2015). However, bubbles in noodle dough have to our knowledge not been a subject of direct observation, perhaps due to their lower concentration (based on density measurements (Bellido & Hatcher, 2010)), but also because noodle doughs are not leavened, as bread dough is, examination of bubbles has not been deemed important. Nevertheless, the presence of bubbles will affect the quality of the manufactured noodles and the texture of the cooked product. Bubbles will also affect noodle dough drying performance and the appearance of the packaged product. As a consequence, an understanding of bubbles and their origin during noodle dough sheet manufacturing is important for optimizing quality for this global food staple.

The objective of this work is to show that noodle dough contains air bubbles whose properties are altered by the manufacturing process. One of the main interests of this work is the use of X-Ray microtomography and powerful image analysis techniques to characterize the distribution and orientation of the bubbles, outcomes that can be used in other food processing applications.

2. Materials and methods

2.1. Materials and sample preparation

A hard red spring wheat flour (made from a blend of Canada Western Red Spring varieties which graded #1 CWRS) was used to prepare noodle dough sheets at 37% water (fwb) absorption with food grade NaCl (1% *w*/w of flour) added as a solution. Doughs were prepared using an asymmetrical speed mixer (Model DAC 150 FV, FlackTec Inc., Landrum, SC), by mixing for 30 s at 3000 rpm in a Pin Max 80 bowl (Hatcher & Preston, 2004).

The mixed dough crumb was subject to one of two laminating (compounding) processes (Hou, 2010; Hou et al., 2010) on a laboratory noodle machine (Ohtake, Tokyo, Japan) with a ten inch diameter pair of rolls at an initial gap setting of 3.0 mm (Salimi-Khorshidi, 2016). After a first lamination step to create a coherent dough sheet from the dough crumb, the dough sheet was folded in half and laminated at the same roll gap (3.0 mm) either once or ten times. For the dough laminated ten times, a 90° rotation was performed at lamination steps 2, 4, 6 and 8, resulting in a dough sheet that was rotated 4 times in total. Following lamination (compounding), dough sheets were submitted to seven reduction passes reducing dough sheet thickness gradually (Hou et al., 2010) by passing through roll gaps from 3.00 mm to 1.10 mm (Table 1). The two noodle dough treatments (referred to as 1lam and 10lam) were therefore different in terms of processing and the amount of work input during processing (Ross & Crosbie, 2010), with control over differences attributable to the number of folding steps occurring during lamination.

Table 1
Sheeting roll gaps for the noodle dough sheet manufacturing process.

Pass number	Reduction roll gap (mm)
1	3.00
2	2.55
3	2.15
4	1.85
5	1.55
6	1.35
7	1.10

Dough sheets were placed in plastic bags and were refrigerated in between experiments. Dough sheet thickness was measured using a caliper prior to experiments in the synchrotron. Dough samples were excised from random locations in the dough sheets: three samples from 10lam, and two samples from 1lam. Analysis of bubble size distributions occurred primarily between 32 and 40 h after noodle dough sheet manufacturing (see Table 2), except for one sample (1lam2).

2.2. Tomography experiments

Experiments were conducted on the Biomedical Imaging and Therapy Facility Insertion Device beamline (BMIT-05ID-2 SOE-1) at the Canadian Light Source (Saskatoon, Saskatchewan). The source is a multi-pole superconducting 4.3 T wiggler. Monochromatic X-rays of 25 keV energy were produced using a bent double-Laue crystal monochromator. (Wysokinski et al., 2015). Filtering of the beam was achieved by inserting an aluminum filter (thickness 1 mm). The detector was an AA-60 beam-monitor with a 10 μm Gadox (Gadolinium oxysulfide) scintillator with a Hamamatsu C9300-124 CCD camera. The pixel size was 8.75 μm/pixel resolution at the scintillator. Preliminary experiments were performed to choose the optimum distance between sample and detector, finally chosen to be 80 cm. A flat-field correction was performed before each noodle dough scan: the flat image (shutter open and no sample) and the dark image (no beam) were taken sequentially in order to correct the background. The dark image measures the electronic background of the CCD. The flat field measures inhomogeneities in the source and effects of all the optics (filters, monochromator, scintillator, detector optics).

For each experiment, the chosen dough sheet was taken out of the fridge, a sample was cut and placed in a circular plastic holder, which was covered with parafilm to prevent moisture loss. The holder was then immediately mounted on the rotation stage in the experimental hutch of the X-ray beamline. Sample scanning involved a rotation through 180° with 0.3° steps at an exposure time of 0.04 s for each X-ray image. A complete scan with data download was performed in 74 s. From the 600 projections (4000 × 248 pixels) obtained with the scan, we performed a reconstruction with NRecon software to get 200 slices (4000 × 4000 pixels) of the noodle dough sample (slice height of 8.75 μm).

2.3. Extracting bubble size distributions

Image analysis was performed with the open source software Fiji (Schindelin et al., 2012), and the “3D Object Counter” (Bolte & Cordelières, 2006) and “BoneJ” Particle Analyzer (Doube et al., 2010) plugins. We chose to analyze a selection of 948 × 948 pixels in the middle of each sample slice in stacks of 120 or 160 slices depending on the sample; for example, accurate assessments of bubble sizes in slices close to the edge are not attainable. On the slices, bubbles were clearly visible (black pixels) and were well separated from the grey background of noodle dough matrix (Fig. 1a and b). After thresholding (Fig. 1c), the bubbly structure of the noodle dough sheet was readily visualized in the image in 3D using Fiji's 3D viewer. An example for a sample that had been laminated once is shown in Fig. 1.

The centre position of each bubble, in x, y and z coordinates, and its volume in voxels were calculated from the binary image stacks (Fig. 1c), using the particle analyzer plugin of Fiji. Bubbles touching the side of the 3D Region Of Interest (ROI) were not taken into account, and a cut-off of 10 voxels (corresponding to 11 μm equivalent radius) was chosen so as to remove objects that were small compared to the resolution limit. More particularly, setting this cut-off removed noise

Table 2
Lognormal distribution characterization parameters for bubble sizes in noodle dough sheets subject to one or ten lamination steps during manufacturing. Standard error (SE) of the fit for median radius, polydispersity ε and mean radius are given, as well as the coefficient of determination R^2. Volume fraction of bubbles is calculated by doing the ratio of total volume occupied by bubbles to the total volume of the region of interest.

Treatment	1lam1	1lam2	10lam1	10lam2	10lam3
Bubble number	10,842	6304	30,891	24,709	25,975
Age	32 h 9 min	51 h 23 min	32 h 47 min	39 h 35 min	39 h 40 min
Median radius	22.3 ± 0.1 μm	21.9 ± 0.1 μm	19.5 ± 0.1 μm	19.2 ± 0.1 μm	18.5 ± 0.2 μm
Polydispersity ε	31.1 ± 0.4%	28.9 ± 0.5%	27.0 ± 0.7%	26.2 ± 0.6%	26.4 ± 0.9%
Mean radius	23.4 ± 0.1 μm	22.9 ± 0.1 μm	20.2 ± 0.2 μm	19.9 ± 0.1 μm	19.2 ± 0.2 μm
Coefficient of Determination R^2	0.9949	0.9914	0.9949	0.9912	0.9816
Volume fraction of bubbles	0.89%	0.62%	1.3%	1.01%	1.0%

from the X-Ray images which produced black dots that would otherwise be considered as bubbles, and which would give rise to erroneous bubble size distributions. In order to calculate an equivalent radius for bubble distribution characterizations, we considered each bubble to be spherical, i.e., size was defined as the radius of a sphere that would contain a volume equivalent to that of the real bubble. Nevertheless, the elongation of the bubbles was also characterized by measuring their actual dimensions.

3. Results and discussion

The microtomography images allow, via careful image analysis, an extensive study of the presence of bubbles, their size and spatial distribution, and their elongation due to the processing of the dough sheet. From a study of two different manufacturing techniques of one unit operation – the sheeting process, the effect that noodle processing has on bubble characteristics within the noodles was observed.

3.1. Bubble size distributions

The bubble equivalent radius distribution was measured for all samples; typical results for both processing regimes (i.e., one lamination step and ten lamination steps) are shown in Fig. 2.

It has been shown that the bubble size distributions in bread dough are well characterized by lognormal distributions (Bellido et al., 2006; Koksel et al., 2016; Shimiya & Nakamura, 1997). The mechanism occluding bubbles in bread dough during mixing of the dough is that air pockets are entrapped and subdivided iteratively into randomly sized bubbles (Campbell, 1991; Shimiya & Nakamura, 1997), with the final volume fraction of bubbles in the dough determined by rates of air entrainment and disentrainment (Chin, Martin, & Campbell, 2004). The high viscosity of the noodle dough (Liao, Chung, & Tattiyakul, 2007), and the fact that most gluten development takes place during laminating and sheeting rather than during mixing (Hou et al., 2010), means that bubbles in noodle dough are not necessarily nucleated by

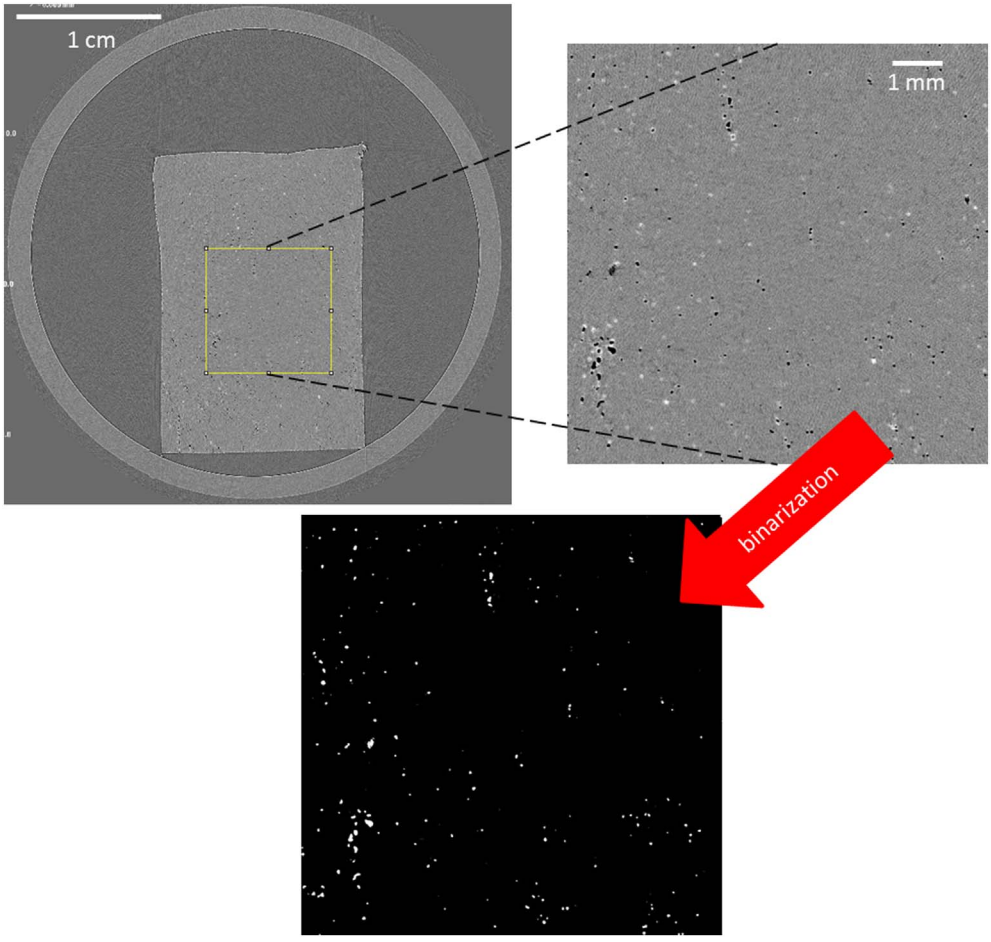

Fig. 1. A region of interest of 948 × 948 pixels is chosen in the image of a noodle dough sheet sample, and a threshold is chosen to binarize the image. This process is repeated for stacks of 120 to 160 image slices.

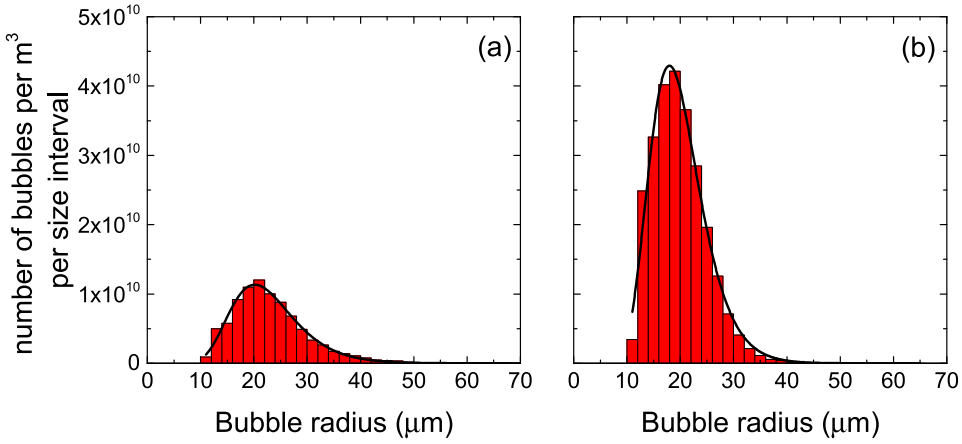

Fig. 2. Typical bubble size distributions in noodle doughs processed with one lamination step (a) and ten laminations (b); solid lines are lognormal fits to the distributions (see Table 2 for fitting parameters).

similar mechanisms to those occurring in bread dough. Nevertheless, the bubble size distributions in noodle dough sheets were all well described by a lognormal distribution probability density function (pdf) given by:

$$f(R) = \frac{1}{\sqrt{2\pi}\,\varepsilon R}\exp\left(\frac{-[ln(R/R_0)]^2}{2\varepsilon^2}\right) \quad (1)$$

where R is bubble radius, R_0 is the median of the lognormal distribution, and ε is the polydispersity of the distribution. The fitting parameters of the lognormal distribution pdf for the samples are summarized in Table 2.

From Fig. 2 and Table 2, it can be seen that the number of lamination steps during manufacturing has a pronounced effect on the bubble size distribution in noodle dough sheets. The total number of bubbles and the volume fraction of bubbles are significantly higher in the ten lamination noodle dough sheets compared to sheets prepared with only one lamination step. Median bubble size and polydispersity are also significantly lower in the noodle dough sheets prepared with ten laminations. Although conventional understanding is that lamination (compounding) "fills in gaps and holes" (Hou et al., 2010; Ross & Hatcher, 2005a; Ross & Hatcher, 2005b), nucleation of bubbles by air entrapment is expected during lamination when the dough sheet is folded in two. The creation of finer, and more numerous, bubbles has been reported for multiple lamination passes of bread dough (Morgenstern, Zheng, Ross, & Campanella, 1999) and pastry dough (Bousquieres, Deligny, Riaublanc, & Lucas, 2014). An illustration of the difference in bubble size distributions according to processing regime is shown in Fig. 3 where typical slice images were extracted from stacks corresponding to the middle (in depth) of the dough sheet.

3.2. Gradient in dough sheet thickness

A gradient in the quantity of bubbles is visible in the xz and yz cuts in Fig. 3, where we see clearly, before image processing, that the number of bubbles is higher in the middle of the thickness of the dough sheets. To investigate quantitatively how the repetitive nature of the lamination process affected the bubble distribution, the distribution within the thickness of the dough sheet was probed. To do so, the data was split along the z-coordinate direction (thickness) to create sections that were 8 slices thick, i.e., 70 μm. For each section, mean bubble equivalent radius, volume fraction, and the total number of bubbles were calculated. Since the analyzed stack of slices was not necessarily in the middle of the noodle dough sheet, a correction for position was added (based on thickness determination from caliper measurements) in order to legitimately compare depth across all samples. The thickness indicated in Figs. 4, 5 and 6 is the real position of sections relative to the bottom surface of the noodle sheet (z = 0).

Bubbles were clearly distributed non-uniformly inside the noodle dough sheets (Fig. 4). In general, their number was higher in the middle of the dough sheet, and this was very evident for noodle doughs made with a greater number of lamination steps. The volume fraction of bubbles was also larger in sheets that were laminated multiple times (Fig. 5). The mean bubble equivalent radius for the dough laminated multiple times, was also larger in the center of the noodle sheet (Fig. 6). More layers of bubbles are potentially created in the ten lamination process vs one layer of bubbles; the lamination (compounding) process

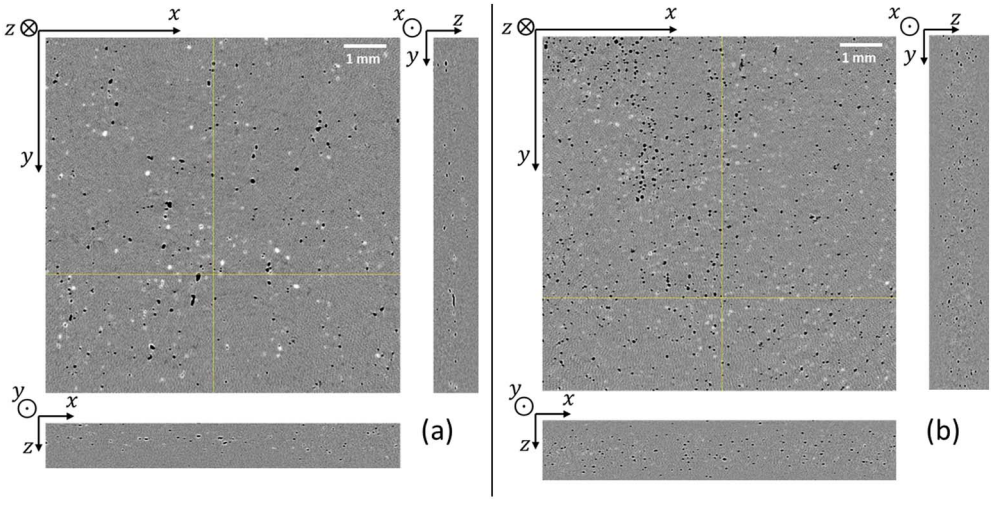

Fig. 3. Slices extracted from the middle of dough sheets processed with one lamination (a) and ten laminations (b). Images on the right and bottom of the xy slices are slices in the yz and xz planes, respectively, extracted along the yellow lines. (For interpretation of the references to color in this figure legend, the reader is referred to the web version of this article.)

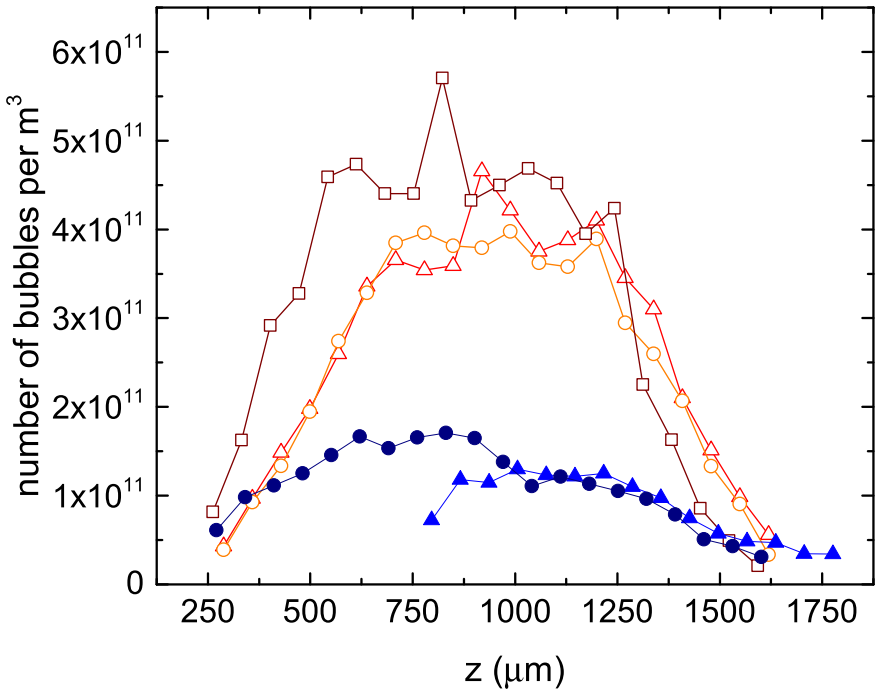

Fig. 4. Number of bubbles per m^3 (70 μm sections) as a function of position in the thickness direction of the noodle sheets. Open symbols: 10 lamination samples, Closed symbols: 1 lamination samples. lam1: ●, lam2: ▲, 10lam1: □, 10lam2: ○, 10lam3: △. Lines are guides for the eye.

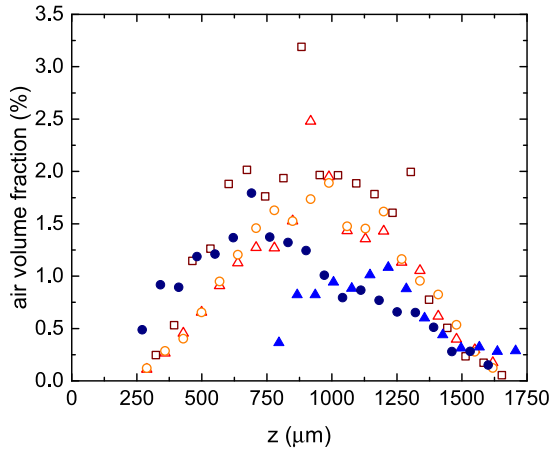

Fig. 5. Air volume fraction in each 70 μm section as a function of position in the thickness dimension of noodle dough sheets processed by different lamination techniques. Open symbols: 10 lamination subsamples, Closed symbols: 1 lamination subsamples. lam1: ●, lam2: ▲, 10lam1: □, 10lam2: ○, 10lam3: △.

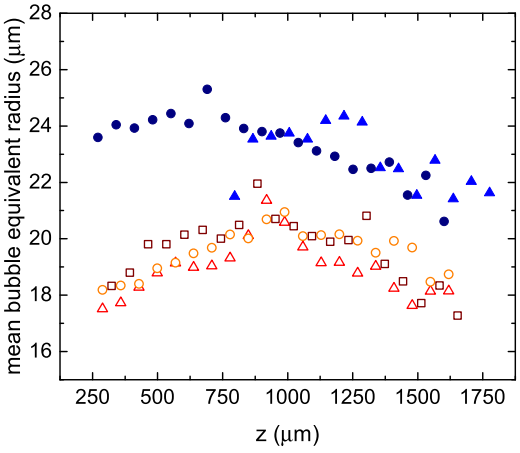

Fig. 6. Mean equivalent radius of bubbles in each 70 μm section as a function of position in the thickness dimension of noodle dough sheets processed by different lamination techniques. Open symbols: 10 lamination samples, Closed symbols: 1 lamination samples. lam1: ●, lam2: ▲, 10lam1: □, 10lam2: ○, 10lam3: △.

is clearly a source of bubble entrapment, and a modification of the bubble distribution.

3.3. Aging of bubbles in noodle doughs

It has been shown that disproportionation is a powerful mechanism changing the bubble size distribution in bread doughs that are made without yeast (Koksel, Scanlon, & Page, 2016). Bubble sizes from Fig. 6 are such that we would expect substantial Laplace-pressure-generated elevations in pressure in the bubbles (van Vliet, 1999), perhaps as large as 7% above atmospheric pressure (from $\Delta P = 2\gamma/R$, where γ is the interfacial tension); this pressure difference will drive disproportionation and so alter bubble sizes in noodle doughs. Two bubble aging phenomena are evident in Table 2 and in Figs. 4-6 that are consistent with changes in bubble numbers and sizes arising from disproportionation.

The gas volume fraction, the number of bubbles and the mean bubble radius decrease as one approaches either surface of the noodle sheet, regardless of the number of laminations. The open atmosphere will act as a sink for gas diffusing out of the bubbles where the gas is at a higher pressure (van Vliet, 1999). Shorter diffusion paths for the gas in bubbles nearer the edge will accelerate shrinkage for the bubbles closer to the edges of the noodle dough sheet (Fig. 6). Loss of gas will be further enhanced if oxygen is consumed in the dough, for example by free fatty acids and polyphenol oxidase (Hatcher, 2010), since this will potentially increase the partial pressure of nitrogen to almost 30% more than the partial pressure of nitrogen in the atmosphere around the noodle dough sheet.

A second factor is the progression in all three bubble parameters (Figs. 4-6) due to delays in analyzing the bubbles tomographically. The number of bubbles decreases with time (Table 2), as expected for processes governed by disproportionation (Meinders & van Vliet, 2004), and in the samples laminated once, where there was a greater delay in analyzing samples compared to the samples laminated ten times, there is a greater percentage drop in bubble numbers (Table 2).

3.4. Bubble orientations

Cursory examination of the tomography images revealed that the bubbles appeared more elongated in the direction of sheeting (y direction in Fig. 3). The effect was more obvious for the sheets laminated only once, where the lamination and elongation due to sheeting are performed in the same direction. The processing used to manufacture the 10 lamination sample involves rotation of the sheet between laminations, followed by elongation steps in one direction. Therefore, if the orientation of bubbles is determined mainly by the lamination process, we would expect to have a more homogeneous orientation of bubbles in the samples processed with ten lamination steps.

We performed a quantitative analysis of bubble orientation using the plugin BoneJ (Doube et al., 2010) in Fiji. To measure any anisotropy of the bubbles in the dough sheet, we used BoneJ to determine the moments of inertia along the short, medium and long axes for each bubble. Although this was conducted for all bubbles, we report results for bubbles with sizes > 97 voxels, even though results for all bubbles are consistent with anisotropy results for the larger bubbles. From the moments of inertia two parameters, flatness and elongation can be defined :

$$\text{Flatness} = \frac{\text{Length of intermediate axis}}{\text{Length of shortest axis}}$$

$$\text{Elongation} = \frac{\text{Length of longest axis}}{\text{Length of intermediate axis}}$$

The results are shown in Table 3. From this, one can see that both lamination processes induced a flattening of the bubbles, and this was slightly more so for bubbles in the noodle doughs subject to one lamination. These flattened bubbles were also elongated, with this elongation being greater for the one lamination process.

By extracting the x, y and z components of the unit vector of the longest principal axis of each bubble in the region of Interest, we can calculate the angles (orientations) of the bubbles relative to the thickness of the sheet and the sheeting direction that corresponded to these anisotropic parameters, flatness and elongation.

From the Cartesian projection with ρ = 1 (unit vector) for each bubble's longest principal axis, angles θ and φ can be recovered for every bubble:

$$\begin{cases} x = \rho \sin\theta \cos\varphi \\ y = \rho \sin\theta \sin\varphi \\ z = \rho \cos\theta \end{cases}$$

The angle θ corresponds to the orientation of the longest principal axis with respect to the thickness of the dough sheet. The histograms in Fig. 7 indicate that regardless of the extent of lamination, this angle was close to 90° with the longest axis almost exclusively located in the horizontal xy planes of the dough sheet. This is not unexpected since we would expect any preferential elongation of bubbles to occur in the plane perpendicular to the roll gap where dough compression takes place (Levine, 1998). CLSM images of pastry dough that was subject to multiple laminations demonstrated that elongation of bubbles occurred in the sheeting direction (Bousquieres et al., 2014).

Table 3
Mean, median and standard deviations (SD) of flatness and elongation for all noodle sheet samples (one lamination or ten laminations) for bubbles larger than 97 voxels.

Subsample	1lam1	1lam2	10lam1	10lam2	10lam3
# of bubbles (> 97 voxels)	3752	2102	5273	3687	3376
Flatness (mean)	1.10	1.13	1.09	1.11	1.10
Flatness (median)	1.10	1.13	1.08	1.11	1.10
Flatness SD	0.05	0.06	0.04	0.05	0.05
Elongation (mean)	1.40	1.43	1.40	1.33	1.36
Elongation (median)	1.28	1.30	1.26	1.19	1.22
Elongation SD	0.36	0.41	0.38	0.37	0.37

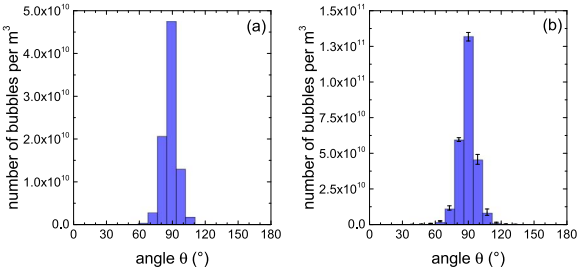

Fig. 7. Distribution of principal axis of orientation along the angle θ, indicating preferential orientation of bubbles at right angles to the roll gap (i.e., flattening in the z axis direction): one lamination (a) and ten laminations (b). Note that the scales on the figures are different. Error bars correspond to the range for two samples.

Although it is quite clear for both lamination treatments that there was no tendency for bubbles to orient in the z direction, the histogram of bubble orientations in the xy plane (angle φ) differs depending on whether the dough was subject to one or ten laminations. A pronounced orientation in the sheeting direction (φ) was observed for dough subject to one lamination with the fewest number of bubbles being oriented perpendicular (within the x-y plane) to the sheeting direction (Fig. 8a). Orientation in the x-y plane was less clear for noodle sheets made with 10 lamination steps. Evidently, dough sheets prepared with multiple perpendicular laminations are a much more homogeneous product.

4. Conclusions

This study clearly demonstrated that noodle doughs contain many bubbles, despite their relatively low volume fraction. Bubble size distributions were well captured by a lognormal distribution. Because the gas volume fraction of multiply-laminated sheets was significantly higher, we conclude that lamination steps entrap bubbles within the dough sheet, and these bubbles are smaller and more homogeneous in size. Bubbles were essentially localized around the centre (in thickness) of the noodle dough sheet, and this was more pronounced for dough sheets prepared with 10 laminations. This is likely associated with bubble aging, due to gas in bubbles close to the surface escaping more readily. The sheeting process that compresses the dough between the rolls, flattens the bubbles and elongates them in the sheeting direction (and this is pronounced for larger than average bubble size). Despite the unidirectional process of sheeting, a persistent effect of lamination history affected the bubble distribution in the final noodle dough sheet. These findings provide a more complete knowledge of the structure of noodle dough sheets, findings that have implications for noodle quality.

Acknowledgements

Research described in this paper was performed at the BMIT facility at the Canadian Light Source, which is supported by the Canada Foundation for Innovation, Natural Sciences and Engineering Research Council of Canada, the University of Saskatchewan, the Government of Saskatchewan, Western Economic Diversification Canada, the National Research Council Canada, and the Canadian Institutes of Health Research. Financial support for this research from NSERC Strategic grant (STPGP 463167 – 14) and Discovery grants (RGPIN/138588-2013), and for research funds from Saskatchewan Agriculture & Food is very much appreciated. The authors would like to thank personnel from the Grain Research Laboratory who supplied the samples, the Canadian Light Source in Saskatoon for the opportunity to perform this study as well as for their great help during the experiments, Andrew Pankewycz for the design and machining of the sample holder, all the team from the University of Saskatchewan who helped during the experimental shiftwork and S. Kerhervé for fruitful discussions and comments.

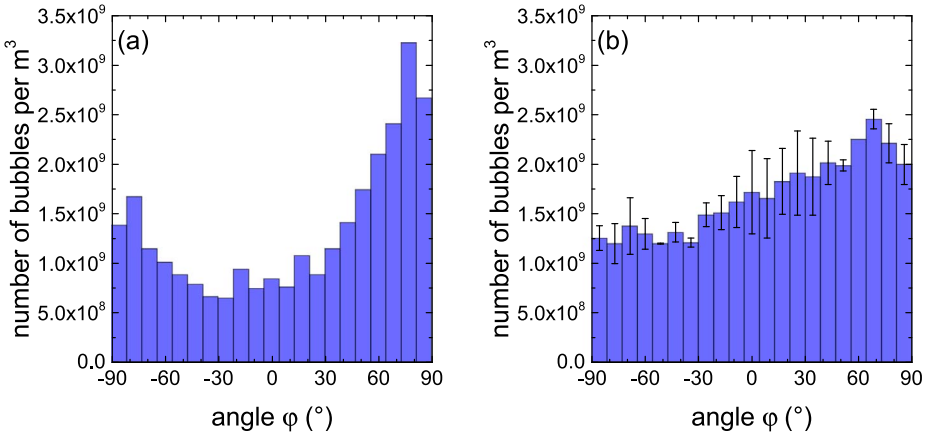

Fig. 8. Distribution of principal axis of orientation along the angle φ, indicating orientation in the xy plane. Dough sheets subject to one (a) or ten (b) laminations prior to sheeting in the y direction for bubbles with a volume larger than 97 voxels (i.e., equivalent radius around 25 μm). Error bars correspond to the range for two samples.

References

Babin, P., Della Valle, G., Dendievel, R., Lourdin, D., & Salvo, L. (2007). X-ray tomography study of the cellular structure of extruded starches and its relations with expansion phenomenon and foam mechanical properties. *Carbohydrate Polymers, 68*(2), 329–340.

Baker, J. C., & Mize, M. D. (1941). The origin of the gas cell in bread dough. *Cereal Chemistry, 18*, 19–34.

Bellido, G. G., & Hatcher, D. W. (2010). Ultrasonic characterization of fresh yellow alkaline noodles. *Food Research International, 43*(3), 701–708.

Bellido, G. G., Scanlon, M. G., Page, J. H., & Hallgrimsson, B. (2006). The bubble size distribution in wheat flour dough. *Food Research International, 39*(10), 1058–1066.

Bolte, S., & Cordelières, F. P. (2006). A guided tour into subcellular colocalization analysis in light microscopy. *Journal of Microscopy, 224*, 213–232.

Bousquieres, J., Deligny, C., Riaublanc, A., & Lucas, T. (2014). CLSM study of layers in laminated dough: Roll out of layers and elastic recoil. *Journal of Cereal Science, 60*, 82–91.

Campbell, G. M. (1991). *The aeration of bread dough during mixing.* Ph.D. ThesisUniversity of Cambridge.

Campbell, G. M., Rielly, C. D., Fryer, P. J., & Sadd, P. A. (1998). Aeration of bread dough during mixing: Effect of mixing dough at reduced pressure. *Cereal Foods World, 43*, 163–167.

Campbell, G. M., Scanlon, M. G., & Pyle, D. L. (2008). *Bubbles in food 2: Novelty, health and luxury.* St. Paul, MN: Eagan Press.

Campbell, G. M., Webb, C., Pandiella, S. S., & Niranjan, K. (1999). *Bubbles in food.* St. Paul, MN: Eagan Press.

Chin, N. L., Martin, P. J., & Campbell, G. M. (2004). Aaeration during bread dough mixing I. Effect of direction and size of a pressure step – Change during mixing on the turnover of gas. *Food and Bioproducts Processing, 82*(C4), 1–7.

Chin, N. L., Martin, P. J., & Campbell, G. M. (2005). Dough aeration and rheology: Part 3. Effect of the presence of gas bubbles in bread dough on measured bulk rheology and work input rate. *Journal of the Science of Food and Agriculture, 85*(13), 2203–2212.

Dawe, P. R., Johnston, K. W., & Dintheer, W. (2001). Pasta mixing and extrusion. In R. C. Kill, & K. Turnbull (Eds.). *Pasta and semolina technology* (pp. 86–118). Oxford: Blackwell Science.

Diep, S., Daugelaite, D., Strybulevych, A., Scanlon, M., Page, J., & Hatcher, D. (2014). Use of ultrasound to discern differences in Asian noodles prepared across wheat classes and between varieties. *Canadian Journal of Plant Science, 94*, 525–534.

Doube, M., Klosowski, M., Arganda-Carreras, I., Cordelières, F., Dougherty, R., Jackson, J., ... Hutchinson, J. (2010). BoneJ: Free and extensible bone image analysis in ImageJ. *Bone, 47*(6), 1076–1079.

Edwards, N. M., Scanlon, M. G., Kruger, J. E., & Dexter, J. E. (1996). Oriental noodle dough rheology: Relationship to water absorption, formulation, and work input during dough sheeting. *Cereal Chemistry, 73*, 708–711.

Falcone, P., Baiano, A., Conte, A., Mancini, L., Tromba, G., Zanini, F., & Del Nobile, M. (2006). Imaging techniques for the study of food microstructure: A review. *Advances in Food and Nutrition Research, 51*(06), 205–263.

Fu, B. X. (2008). Asian noodles: History, classification, raw materials, and processing. *Food Research International, 41*, 888–902.

Hatcher, D. W. (2010). Objective evaluation of noodles. In G. G. Hou (Ed.). *Asian noodles science, technology, and processing* (pp. 227–249). Hoboken, NJ: Wiley.

Hatcher, D. W., & Anderson, M. J. (2007). Influence of alkaline formulation on oriental noodle color and texture. *Cereal Chemistry, 84*, 253–259.

Hatcher, D. W., Bellido, G. G., & Anderson, M. J. (2009). Flour particle size, starch damage, and alkali reagent: Impact on uniaxial stress relaxation. *Cereal Chemistry, 86*(3), 361–368.

Hatcher, D. W., & Preston, K. P. (2004). Investigation of a small-scale asymmetric centrifugal mixer for the evaluation of Asian noodles. *Cereal Chemistry, 81*, 303–307.

Hatcher, D. W., Salimi, A., Daugelaite, D., Strybulevych, A., Scanlon, M. G., & Page, J. H. (2014). Application of ultrasound to the evaluation of rheological properties of raw Asian noodles fortified with barley beta-glucan. *Journal of Texture Studies, 45*, 220–225.

Hou, G. G. (2010). Laboratory pilot-scale Asian noodle manufacturing and evaluation protocols. In G. G. Hou (Ed.). *Asian noodles science, technology, and processing* (pp. 183–225). Hoboken, NJ: Wiley.

Hou, G. G., Otsubo, S., Okuso, H., & Shen, L. (2010). Noodle processing technology. In G. G. Hou (Ed.). *Asian noodles science, technology, and processing* (pp. 99–140). Hoboken, NJ: Wiley.

Inazu, T., Iwasaki, K., & Furuta, T. (2005). Stress and crack prediction during drying of Japanese noodle (udon). *International Journal of Food Science and Technology, 40*, 621–630.

Johnston, K. W., & Dintheer, W. (2001). Pasta drying. In R. C. Kill, & K. Turnbull (Eds.). *Pasta and Semolina Technology* (pp. 158–175). Oxford: Blackwell Science.

Koksel, F., Aritan, S., Strybulevych, A., Page, J., & Scanlon, M. (2016a). The bubble size distribution and its evolution in non-yeasted wheat flour doughs investigated by synchrotron X-ray microtomography. *Food Research International, 80*, 12–18.

Koksel, F., Scanlon, M. G., & Page, J. H. (2016b). Ultrasound as a tool to study bubbles in dough and dough mechanical properties: A review. *Food Research International, 89*, 74–89.

Levine, L. (1998). Models for dough compressibility in sheeting. *Cereal Foods World, 43*(8), 629–634.

Li, M., Zhu, K. X., Peng, J., Guo, X. N., Amza, T., Peng, W., & Zhou, H. M. (2014). Delineating the protein changes in Asian noodles induced by vacuum mixing. *Food Chemistry, 143*, 9–16.

Li, M., Zhu, K. X., Sun, Q.-J., Amza, T., Guo, X. N., & Zhou, H. M. (2016). Quality characteristics, structural changes, and storage stability of semi-dried noodles induced by moderate dehydration. Understanding the quality changes in semi-dried noodles. *Food Chemistry, 194*, 797–804.

Liao, H.-J., Chung, Y.-C., & Tattiyakul, J. (2007). Biaxial extensional viscosity of sheeted noodle dough. *Cereal Chemistry, 84*(5), 506–511.

Liu, R., Xing, Y., Zhang, Y., Zhang, B., Jiang, J., & Wei, Y. (2015). Effect of mixing time on the structural characteristics of noodle dough under vacuum. *Food Chemistry, 188*, 328–336.

Meinders, M. B. J., & van Vliet, T. (2004). The role of interfacial rheological properties on Ostwald ripening in emulsions. *Advances in Colloid and Interface Science, 108–109*, 119–126.

Mercier, S., Mondor, M., Moresoli, C., Villeneuve, S., & Marcos, B. (2016). Drying of durum wheat pasta and enriched pasta: A review of modeling approaches. *Critical Reviews in Food Science and Nutrition, 56*(7), 1146–1168.

Miskelly, D. M., & Moss, H. J. (1985). Flour quality requirements for Chinese noodle manufacturer. *Journal of Cereal Science, 3*, 379–387.

Morgenstern, M. P., Zheng, H., Ross, M., & Campanella, O. H. (1999). Rheological properties of sheeted wheat flour dough measured with large deformations. *International Journal of Food Properties, 2*(3), 265–275.

Ross, A. S. (2006). Instrumental measurement of physical properties of cooked Asian wheat flour noodles. *Cereal Chemistry, 83*(1), 42–51.

Ross, A. S., & Crosbie, G. B. (2010). Effects of flour characteristics on noodle texture. In G. G. Hou (Ed.). *Asian noodles science, technology, and processing* (pp. 313–329). Hoboken, NJ: Wiley.

Ross, A. S., & Hatcher, D. W. (2005a). Guidelines for the laboratory manufacture of Asian wheat flour noodles. *Cereal Foods World, 50*(6), 296–304.

Ross, A. S., & Hatcher, D. W. (2005b). Navigating noodle texture: Taking the rheological route. *Cereal Foods World, 61*(3), 92–95.

Salimi-Khorshidi, A. (2016). *Use of ultrasound to determine the effects of sheeting work input and barley β-glucan addition on mechanical properties of Asian noodles (PhD dissertation).*

Scanlon, M. G., & Zghal, M. C. (2001). Bread properties and crumb structure. *Food Research International, 34*, 841–864.

Schindelin, J., Arganda-Carreras, I., Frise, E., Kaynig, V., Longair, M., Pietzsch, T., & Cardona, A. (2012). Fiji: An open-source platform for biological-image analysis. *Nature Methods, 9*(7), 676–682.

Shimiya, Y., & Nakamura, K. (1997). Changes in size of gas cells in dough and bread during breadmaking and calculation of critical size of gas cells that expand. *Journal of Texture Studies, 28*(3), 273–288.

Smewing, J. (2016). Navigating noodle texture: Taking the rheological route. *Cereal Foods World, 61*(3), 92–95.

Turbin-Orger, A., Babin, P., Boller, E., Chaunier, L., Chiron, H., Della Valle, G., ... Salvo, L. (2015). Growth and setting of gas bubbles in a viscoelastic matrix imaged by X-ray microtomography: The evolution of cellular structures in fermenting wheat flour dough. *Soft Matter, 11*, 3373–3384.

van Vliet, T. (1999). Physical factors determining gas cell stability in a dough during bread making. In G. M. Campbell, C. Webb, S. S. Pandiella, & K. Niranjan (Eds.). *Bubbles in food* (pp. 121–127). St. Paul, MN: Eagan Press.

Wysokinski, T., Chapman, D., Adams, G., Renier, M., Suortti, P., & Thomlinson, W. (2015). Beamlines of the biomedical imaging and therapy facility at the Canadian Light Source – Part 3. *Nuclear Instruments and Methods in Physics Research A, 775*(1), 1–4.